# TRIAXIALITY EFFECTS ON HYDROGEN-ASSISTED MICRO-DAMAGE EVOLUTION IN EUTECTOID STEEL

J. TORIBIO and E. VASSEUR
*Department of Materials Science, University of La Coruña*
*E.T.S.I. Caminos, Campus de Elviña, 15192 La Coruña, Spain*

## ABSTRACT

This paper offers a detailed analysis of the hydrogen-assisted micro-damage region in axisymmetric round-notched samples of high-strength eutectoid steel under hydrogen embrittlement environmental conditions. Emphasis is placed on the microscopic appearance and the evolution of such a microscopic topography from the initiation (sub-critical) to the fracture (critical) point. The use of very different notched geometries —with the subsequent various triaxial stress distributions in the vicinity of the notch tip— allows an analysis of the influence of stress state on hydrogen diffusion and micro-cracking. In all cases, the microscopic appearance of the hydrogen-affected zone resembles micro-damage, micro-cracking or micro-tearing due to hydrogen degradation.

## KEYWORDS

Hydrogen-assisted micro-damage, pearlitic steel, tearing topography surface.

## INTRODUCTION

Hydrogen-assisted fracture is usually associated with a sort of hydrogen-induced damage at the microscopical level (Kim and Morris, 1983). In eutectoid steel such a region is the so called *tearing topography surface* or TTS (Toribio *et al.*, 1991a), whose extension is related to the testing variables governing the phenomenon.

This paper is focussed on the influence of the stress state in the vicinity of the notch on the microscopic appearance and progression of the TTS region from the initiation (sub-critical) to the fracture (critical) point, to elucidate some specific features of the evolution of this hydrogen-affected region throughout fracture tests under hydrogen environment in a triaxial stress state produced by a notch.

## EXPERIMENTAL PROGRAMME

The material used in this investigation was a hot rolled pearlitic steel supplied from commercial stock by *Nueva Montaña Quijano Company* (Santander, Spain), in bar

form of 12 mm diameter. Chemical composition and mechanical properties appear in Tables 1 and 2 respectively.

Table 1. Chemical composition (wt%)

| C | Mn | Si | P | S |
|---|---|---|---|---|
| 0.85 | 0.60 | 0.26 | 0.010 | 0.030 |

Table 2. Mechanical properties

| E (GPa) | $\sigma_Y$ (MPa) | $\sigma_{max}$ (MPa) | $\varepsilon(\sigma_{max})$ (%) | P (MPa) | n |
|---|---|---|---|---|---|
| 199 | 600 | 1151 | 6.1 | 2100 | 4.9 |

*P,n: Ramberg-Osgood Parameters:* $\varepsilon = \sigma/E + (\sigma/P)^n$

The stress-strain curve of the steel appears in Fig. 1, together with the Ramberg-Osgood modelling used in the numerical computations. Four notched geometries were used of different depth and radii, as sketched in Fig. 2, so as to achieve very different constraint situations in the vicinity of the notch tip.

The samples were subjected to slow strain rate testing with displacement rates between $10^{-10}$ and $2.10^{-6}$ m/s. The test environment was an aqueous solution of 1 g/l calcium hydroxide plus 0.1 g/l sodium chloride. The pH value was 12.5 and tests were performed at constant potential of –1200 mV SCE.

## FRACTOGRAPHIC ANALYSIS

Hydrogen-assisted micro-damage started at the notch tip, and SEM fractographic analysis showed a characteristic microscopic fracture mode with a kind of ductile tearing appearance: the so called *tearing topography surface* or TTS, following Thompson and Chesnutt (1979). It appears only under cathodic potentials (Toribio *et al,* 1991a), its size increases clearly as the potential becomes more negative and slightly as the pH decreases (Toribio *et al.*, 1991b). It resembles micro-damage due to hydrogen (Toribio *et al.*, 1991b), which agrees with previous research (Keefe *et al.*, 1984) and it can be viewed as a slow crack growth topography associated with the stage II or *plateau* in the crack growth kinetics curve (Toribio *et al,* 1991a), which is consistent with other works (Lee *et al.*, 1991). In addition, the TTS size decreases with the strain rate and with the maximum fatigue precracking load in precracked samples (Toribio *et al.*, 1992), and it is clearly influenced by the geometry in notched samples, reaching the location of the maximum hydrostatic stress point in quasi-static tests (Toribio *et al.* , 1992), which is consistent with a mechanism of hydrogen diffusion.



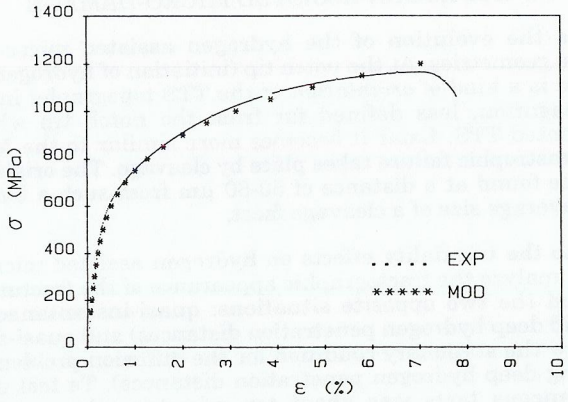


Fig. 1. Stress-strain curve of the steel and Ramberg-Osgood modelling used in the numerical computations.

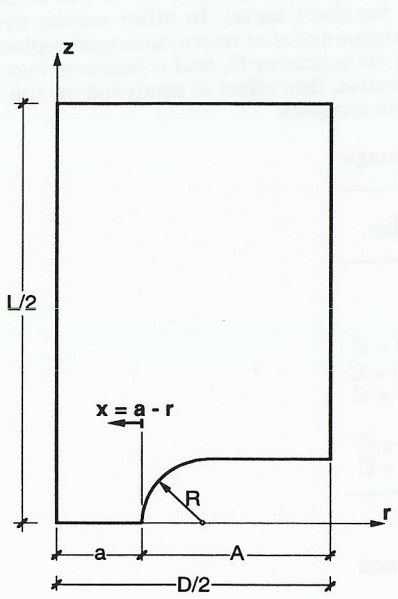


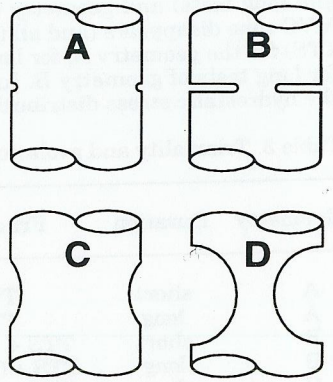


| Sample | R/D | A/D |
|---|---|---|
| A | 0.03 | 0.10 |
| B | 0.05 | 0.39 |
| C | 0.36 | 0.10 |
| D | 0.40 | 0.39 |

Fig. 2. Notched geometries used in the experimental programme.where R is the notch radius, A the notch depth and D the diameter of the sample (D = 11.25 mm for all specimens, after machining).

## EVOLUTION OF HYDROGEN-ASSISTED MICRO-DAMAGE

Fig. 3. shows the evolution of the hydrogen assisted micro-damage in two representative geometries. At the notch tip (initiation of hydrogen-assisted micro-damage) there is a kind of *orientation* of the TTS topography in the direction of damage propagation, less defined far from the notch tip where it becomes randomly-oriented TTS. Later it becomes more similar to the MVC topography and finally catastrophic failure takes place by cleavage. The origin of the cleavage fracture can be found at a distance of 50-60 μm from such a boundary, i.e., the approximate average size of a cleavage facet.

With regard to the triaxiality effects on hydrogen assisted micro-damage, it is interesting to analyze the fractographic appearance of the fracture surface for all geometries and the two opposite situations: quasi-instantaneous tests (short enough to avoid deep hydrogen penetration distances) and quasi-static tests (long enough to allow the stationary condition for the diffusion problem to be reached, thus permitting deep hydrogen penetration distances). Te test duration for the quasi-instantaneous tests was about ten minutes, whereas for quasi-static experiments it ranged from ten to fifty hours.

Table 3 gives the evolution of damage for different triaxiality situations. The transition zone between the TTS and the cleavage-like topography in the form of quasi-MVC surface appears only in certain cases: geometries B and D (for short and long tests) and geometry C (only for short tests). In other words, the quasi-MVC zone disappears (and all the hydrogen-assisted micro-damaged region is pure TTS) for the geometry A, for long tests on geometry C, and it becomes less defined for long tests of geometry B. In next section this effect is analyzed on the basis of the hydrostatic stress distribution in the samples.

Table 3. Triaxiality and evolution of damage

| Geometry | Duration | Fractography |
|---|---|---|
| A | short | TTS + C |
| A | long | TTS + C |
| B | short | TTS + QMVC + C |
| B | long | TTS + (QMVC) + C |
| C | short | TTS + QMVC + C |
| C | long | TTS + C |
| D | short | TTS + QMVC + C |
| D | long | TTS + QMVC + C |

*TTS: Tearing Topography Surface*
*QMVC: Quasi Micro-Void Coalescence*
*(QMVC): Idem, when it is short or ill-defined*
*C: Cleavage-like*

## CONTINUUM MECHANICS APPROACH

Hydrostatic stress plays an important role in hydrogen transport (Toribio *et al.*, 1991c) and thus the hydrostatic stress distributions in the samples were obtained



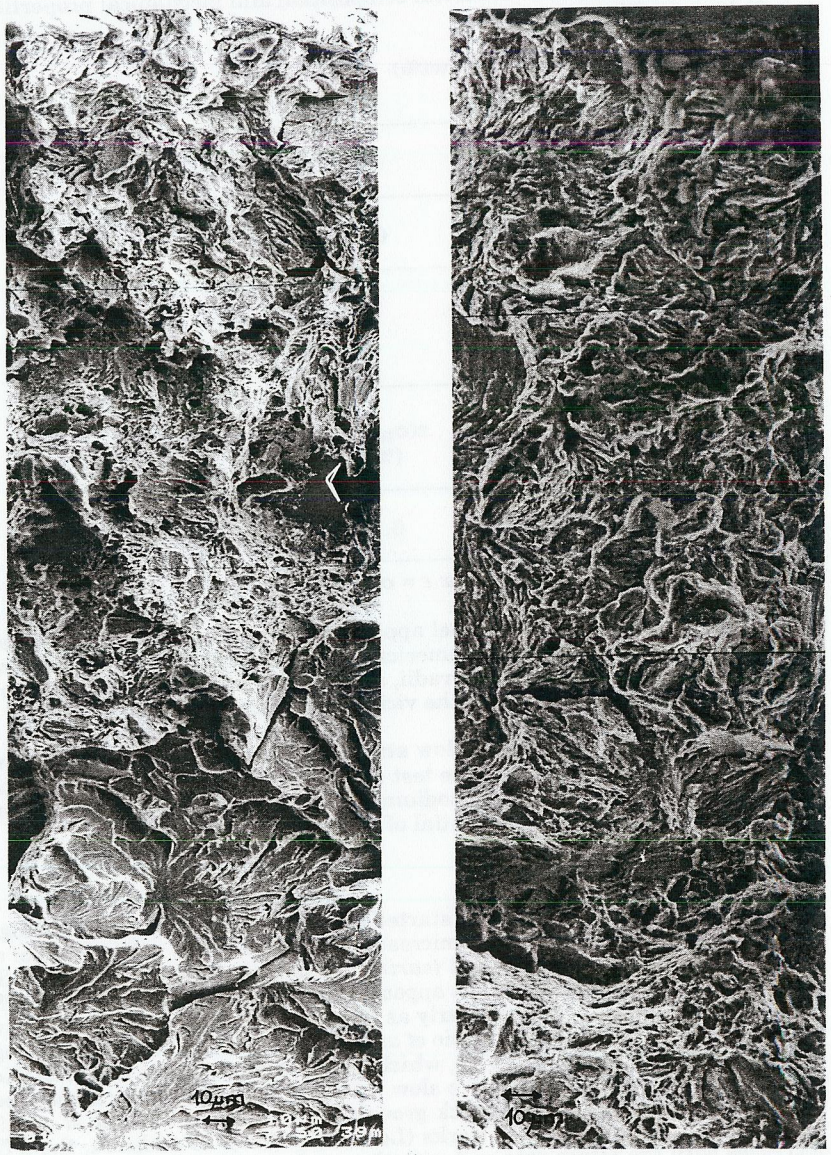


Fig. 3. Evolution of hydrogen assisted micro-damage: (a) left, geometry B, 12 min; progress from pure TTS to cleavage-like; (b) right, geometry D, 2.5 hours; progress from pure TTS to quasi-MVC. The notch tip is at the top in both cases.

by a numerical procedure. The finite element method (FEM) with an elastic-plastic code was applied, using a Von Mises yield surface with an incompressible constitutive equation (classical plasticity).

The material model used in the computations corresponds to the real high strength steel used in the experimental programme, whose stress-strain curve was introduced into the computer program by means of the Ramberg-Osgood equation whose graphical representation is plotted in Fig. 1.

The external load was applied step by step, in the form of nodal displacements. An improved Newton-Raphson method was adopted, which modified the tangent stiffness matrix at each step. The finite elements used in the computations were isoparametric with second-order interpolation.

The elastic-plastic FEM analysis also demonstrated that the hydrostatic stress levels changed with the loading process, but the point of maximum hydrostatic stress always remains at depth $x_S$ (characteristic of the geometry) from the notch tip, as reported by Toribio *et al.*, 1991c) Fig. 4 gives typical hydrostatic stress distributions in the samples (only the lines of constant hydrostatic stress are shown, but not the numerical values which obviously increase with the external load applied on the sample). For the geometries B and D the maximum hydrostatic stress point is placed at the centre of the net section (the bar axis) and hydrogen is "pumped" towards this point by long-term stress-assisted diffusion.

## DISCUSSION

The quasi-MVC topography appears only when the penetration path for the hydrogen (given by the depth of the maximum hydrostatic stress point) is long if compared with the duration of the tests, i.e., when the hydrogen does not have enough time to reach such a critical point. This seems to demonstrate that the MVC area is a candidate to TTS zone which does not reach such a condition because of an insufficient level of hydrogenation. It could explain the process of hydrogen-assisted micro-damage and whether the MVC area is previous to the TTS zone or posterior to it.

A plausible explanation of the phenomenon on the basis of a *previous* MVC formation could be the following. Firstly, microvoids are initiated in weakly-hydrogenated areas by a mechanism of hydrogen enhanced nucleation, followed by later growth. When an area becomes strongly-hydrogenated, new dimples are nucleated so that the holes are even closely spaced, which progressively produces a TTS feature under a stronger hydrogen influence associated with this final growth or link-up phase (cf. Garber *et al.*, 1981; Park and Thompson, 1990). When hydrogen-assisted micro-damage progresses enough to allow the macroscopic fracture condition to be reached, final fracture takes place by cleavage and the pre-damaged areas weakly hydrogenated do not have enough time to complete the transit to TTS appearance, whereas those areas scarcely hydrogenated simply cleave when the stress concentration is high enough, so that final fracture proceeds with no need of environmental assistance.

The MVC area cannot appear after the TTS since the latter can be analyzed in fracture mechanics terms as a macroscopic crack (produced by hydrogen-assisted micro-damage) prolonging the original notch and greatly increasing the triaxiality level as a consequence of its sharp border. It has been demonstrated in previous



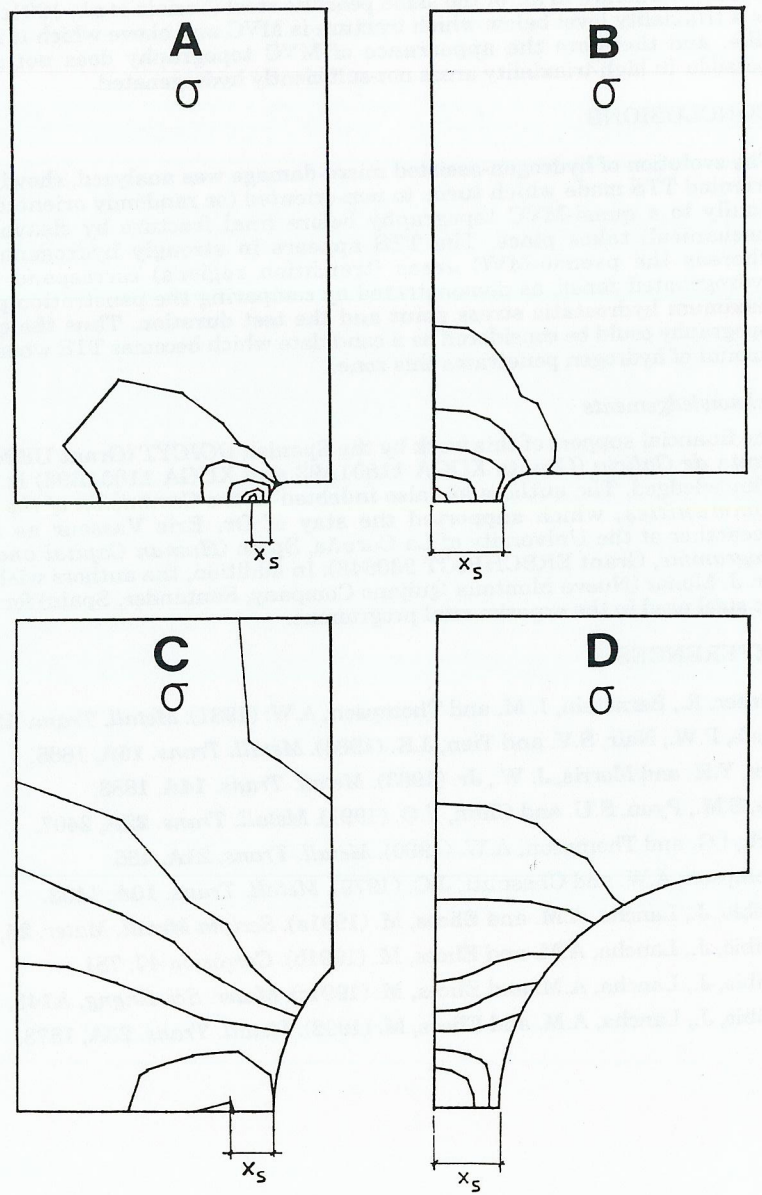


Fig. 4. Distributions of hydrostatic stress in the samples (after numerical analysis).

works on fracture in air of the same pearlitic steel (Toribio *et al.*, 1991c) that there is a triaxiality level below which fracture is MVC and above which it is cleavage-like, and therefore the appearance of MVC topography does not seem to be possible in high-triaxiality areas not-sufficiently hydrogenated.

## CONCLUSIONS

The evolution of hydrogen-assisted micro-damage was analyzed, showing a firstly oriented TTS mode which turns to non-oriented (or randomly oriented) TTS and finally to a quasi-MVC topography before final fracture by cleavage (purely mechanical) takes place. The TTS appears in strongly hydrogenated areas, whereas the pseudo-MVC areas (transition regions) correspond to weakly hydrogenated zones, as demonstrated by comparing the penetration path to the maximum hydrostatic stress point and the test duration. Thus the quasi-MVC topography could be considered as a candidate which becomes TTS when sufficient amount of hydrogen penetrates this zone.

*Acknowledgements*

The financial support of this work by the Spanish *DGICYT* (Grant UE94-001) and *Xunta de Galicia* (Grants XUGA 11801A93 and XUGA 11801B95) is gratefully acknowledged. The authors are also indebted to the *Commision of the European Communities*, which supported the stay of Dr. Eric Vasseur as a visiting researcher at the University of La Coruña, Spain (*Human Capital and Mobility Programme*, Grant ERBCHBICT 930848). In addition, the authors wish to thank Mr. J. Monar (Nueva Montaña Quijano Company, Santander, Spain) for providing the steel used in the experimental programme.

## REFERENCES

Garber, R., Bernstein, I. M. and Thompson, A.W. (1981). *Metall. Trans.* **12A**, 225.

Keefe, P.W., Nair, S.V. and Tien, J.K. (1984). *Metall. Trans.* **15A**, 1865.

Kim, Y.H. and Morris, J. W., Jr. (1983). *Metall. Trans.* **14A**, 1883.

Lee, S.M., Pyun, S.U. and Chun, Y.G. (1991). *Metall. Trans.* **22A**, 2407.

Park, I.G. and Thompson, A.W. (1990). *Metall. Trans.* **21A**, 465.

Thompson, A.W. and Chesnutt, J.C. (1979). *Metall. Trans.* **10A**, 1193.

Toribio, J., Lancha, A.M. and Elices, M. (1991a). *Scripta Metall. Mater.* **25**, 2239.

Toribio, J., Lancha, A.M. and Elices, M. (1991b). *Corrosion* **47**, 781.

Toribio, J., Lancha, A.M. and Elices, M. (1991c). *Mater. Sci. Engng.* **A145**, 167.

Toribio, J., Lancha, A.M. and Elices, M. (1992). *Metall. Trans.* **23A**, 1573.